

Dear Referee #1

We're grateful for your comments and here are our responses to your comments. Our responses to each comment are written with blue-colored texts.

Page 1, Lines 19-22: The sentence should be moved to the first part of paragraph. 2.

- Thanks for your comment, but we decided to put that sentence as it is after careful deliberation. Because we need to provide a background information on how meteor trails to be produced in the introduction as several previous studies did [Lee et al., 2013; Younger et al., 2014].

#### References

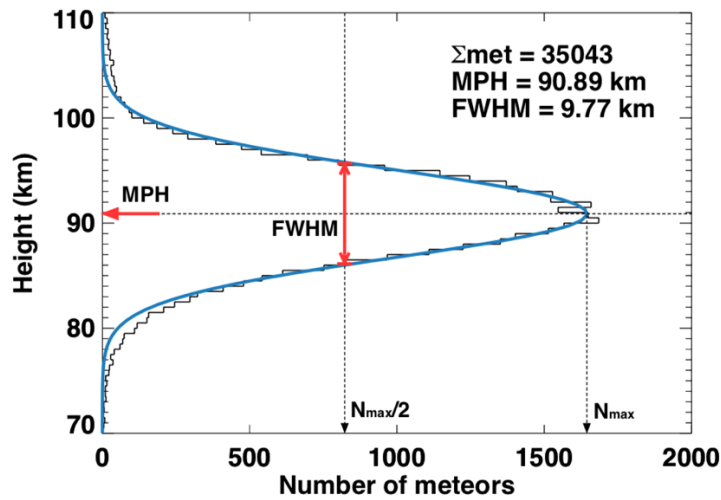
1. Lee, C. S., Younger, J. P., Reid, I. M., Kim, Y. H. and Kim, J. H.: The effect of recombination and attachment on meteor radar diffusion coefficient profiles, *J Geophys Res-Atmos*, 118(7), 3037–3043, doi:10.1002/jgrd.50315, 2013.
2. Younger, J. P. C. S. L. I. M. R. R. A. V. Y. H. K. A. D. J. M.: The effects of deionization processes on meteor radar diffusion coefficients below 90 km,, 1–17, doi:10.1002/(ISSN)2169-8996, 2014.

Page 2, Liu et al. (Liu, L., H. Liu, H. Le, Y. Chen, Y.-Y. Sun, B. Ning, L. Hu, W. Wan, N. Li, and J. Xiong (2017), Mesospheric temperatures estimated from the meteor radar observations at Mohe, China, *J. Geophys. Res. Space Physics*, 122, 2249–2259, doi:10.1002/2016JA023776.) should be cited (reasons will be stated below.).

- We'll added that paper as reference. Thanks.

3. Page 2, Lines 10-11: Since the MHC effect, how to describe the height distribution now because the normal distribution be fail? I am curious at that they still use Guassian function to fit the distribution (Line 21, Page 3) if the MHC effect is important.

- As you pointed out, the meteor radar observation at high altitude is affected by MHC effect and this makes asymmetry in the meteor height distribution as shown in the figure below. However, the extent of the asymmetry is not very severe and the Gaussian function is still the suitable model to determine the best FWHM values to be compared to the SABER temperature.



[Lee et al., 2016]

4. Page 2, Line 8: “invariance” must be deleted, because it is not so as this work presents.

- This study presents the linear relationship between SABER temperature and FWHM based on the fact that the meteor height distribution is primarily controlled by the background atmospheric pressures as shown in Figure 1. The proportionality constant between temperature and FWHM is defined to be a constant as in the equation (3), which was demonstrated from the observational data within measurement errors over the 5-year period as shown in Table 1 in the manuscript. And this is the key idea of the temperature estimation procedure using the observed FWHM, instead of using diffusion coefficient. Once it is determined from the independent measurements such as SABER in our study, the daily mean temperature can be estimated from the meteor radar observed FWHM alone without any additional information.

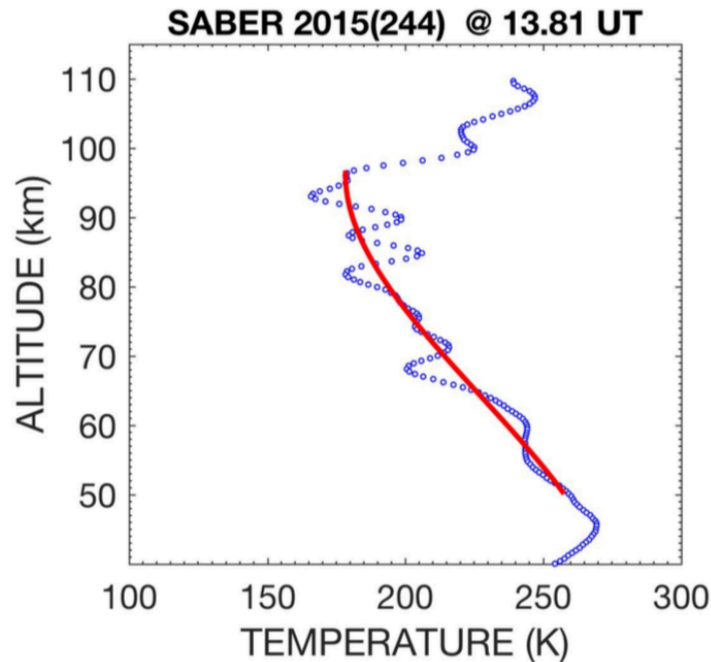
5. Page 3, Lines 1-2: Since there are so limited observations from SABER over the station (the authors can check the local time coverage of SABER), how can they obtain information of geopotential height at times without SABER passes.

- We agree that the SABER only scan two local times over one local position a day as it has a sun synchronous orbit but, we don't need SABER data to get geopotential height from the meteor echo data. There is a simple equation to convert between the geometric height (h) and geopotential height (hg) as follows,  

$$hg = h * (r / (r - h))$$

where r is the earth's radius. Based on this formula, all the geometric heights of meteor echo can be easily converted to geopotential height without SABER data.

6. As Figure shown below for example,



the authors should be stated clearly step by step in the revised manuscript how to obtain the layer mean temperature from SABER. As there are waves in the temperature profile, how to take them into account to get the background profile?

- Since the accumulated meteor height distribution during a day only provides one FWHM, it is more natural that the FWHM can reflect the daily mean temperature not the temperature at the moment. The layer mean temperature corresponds to the red solid line (of course there is height-bin dependence) and the red solid line still shows mean temperature information even if there is a wave structure in the profile. Daily mean temperature can be obtained by averaging the at least two individual temperature profiles (your figure is a single temperature profile at 13.81 UT) and wave structures is more likely getting weaker or even smoothed out in the average procedure.

7. More important, the SABER temperature lacks local time coverage, how to obtain daily mean temperature. If it fails to do so, how to reach the statement as given in Page 2, Lines 8-9.

- Since the SABER only covers two separated local times (day and night for each) over any geographic locations, we calculated mean temperature profile from the SABER temperature data recorded on a single day of year. Several previous studies [Meek et al., 2013; Holmen et al., 2016; Yi et al., 2016] used spatial grid to limit MLS or SABER temperature to the specific location for direct comparison with local meteor radar data and we also did in the same way. Determining the spatial grid for data selection is a tradeoff between number of available satellite data and accurate comparison with the local ground-based

measurement.

#### References

1. Meek, C. E., Manson, A. H., Hocking, W. K. and Drummond, J. R.: Eureka, 80° N, SKiYMET meteor radar temperatures compared with Aura MLS values, *Annales Geophysicae*, 31(7), 1267–1277, doi:10.5194/angeo-31-1267-2013, 2013.
2. Holmen, S. E., Hall, C. M. and Tsutsumi, M.: Neutral atmosphere temperature trends and variability at 90 km, 70°N, 19°E, 2003–2014, *Atmos. Chem. Phys.*, 16(12), 7853–7866, doi:10.5194/acp-16-7853-2016, 2016.
3. Yi, W., Xue, X., Chen, J., Dou, X., Chen, T. and Li, N.: Estimation of mesopause temperatures at low latitudes using the Kunming meteor radar, *Radio Sci.*, 51(3), 130–141, doi:10.1002/2015RS005722, 2016.

8. Page 3, Lines 15-16, describe the daily profile number of SABER available over the station.

- When we limit SABER data to the distance of less than 500 km from the location of KSS, 3-4 profiles are available on average.

9. Page 4, Lines 20-21: It must be deleted, because Equation (1) is not valid under this case. In other words, the authors should be realized that there are assumptions being made.

- The thermodynamic state of the atmosphere at any point is determined by pressure, temperature and density. These variables are related to each other by the ideal gas law. The hydrostatic balance provides an excellent approximation for the vertical dependence of the pressure field in the real atmosphere [Andrew et al., 1987; Holton, 2004; North et al., 2014]. Of course the real atmosphere is different from its ideal state but they work very well. Below references obviously show that ideal gas law and hydrostatic equation can be used to describe atmospheric physics. It would be appreciated if you provide more appropriate equations better describing the FWHM and atmospheric pressure field than equation (1).

#### References

1. Andrew, D. G., Holton, J. R., Leovy, C. B., *Middle Atmospheric Dynamics*, Academic Press. 1987.
2. Holton, J. R., *An introduction to dynamic meteorology*, vol. 88, Academic Press, 2004.
3. North, G. R., Pyle, J. A. and Zhang, F.: *Encyclopedia of Atmospheric Sciences*, Elsevier. 2014.

10. Page 4, Lines 24-25: It should be removed as reason being given in the above and also in the Table.

- As we already mentioned in previous response to comment 4, time-invariance of proportionality constant is a fundamental idea to make the FWHM estimate background atmospheric temperature. Otherwise whenever we determine the atmospheric temperature from the FWHM, we need SABER or MLS temperatures to conduct linear regression procedure. This study wants to tell that the temperature can be estimated from the FWHM alone without any further information. The proportionality constant in the table has its own standard error due to uncertainties in FWHM and SABER temperature measurements, please note that the constant does not change within a given standard errors during the entire periods.

11. Page 4, Lines 25-31: Words are required to tell how to get such result.

- Firstly, we try to find the two height layers where the envelopes of the FWHM meet (please refer to figure 1 in the manuscript) and SABER pressure values at those two height layers can be found every day. Once two pressure values over the entire observational period are recorded, we calculate mean value of two pressures (P1, P2) and they can be used to obtain the proportionality constant from  $C = \frac{g}{R} \left[ \ln \left( \frac{P_1}{P_2} \right) \right]^{-1}$

12. Page 5, Lines 3-5: no ideal local time coverage is reached for the SABER observations, how to get FWHM with geopotential height information from SABER and layered mean temperature? Figure is welcome to show it.

- We already mentioned how to get geopotential height without SABER data in our response to comment 5. All the geometric height of meteor echo data can be converted to geopotential height using a simple formula.

13. Page 5, Lines 20-23: the statement is invalid, because geopotential height of each echo should be given and the ratio of layer mean temperature to FWHM be given.

- From the simple relation in our response to comment 5 between the geometric and geopotential height we already obtained all the geopotential height from the meteor echo data. Based on the linear relationship between the FWHM and the temperature,  $T = C \cdot \text{FWHM}$ , we can calculate the daily mean temperature directly using FWHM alone. Lee et al., (2016) already showed that FWHM can provide better temperature estimation with lower uncertainties than meteor decay times.

#### Reference

Lee, C., Kim, J. -H., Jee, G., Lee, W., Song, I. S. and Kim, Y. H., New method of estimating temperatures near the mesopause

region using meteor radar observations, *Geophys. Res. Lett.*, 43(2), 10, doi:10.1002/2016GL071082, 2016.

14. Page 5, Lines 30-32: It is not the same in the height range as FWHM covered. If the statement here is true, what is usefulness of Equations (1)-(3).

They are no the same now. Further, how to understand the result presented in Figure 3. I now strongly feel the authors make the layer mean temperature over FWHM and temperature at specific height confusing (although they may mean the temperature within 2.4 km).

- According to your comment, we'll add more description in data analysis part for better understanding about the layer mean temperature. All the equations are essential to approve the linear relationship between the FWHM and background temperature based on the fact that the FWHM corresponds to the height difference between two fixed atmospheric pressures as shown in figure 1 in the manuscript. When we compare the proportionality constant from the least-squares fitting with one from the equation  $C = \frac{g}{R} \left[ \ln \left( \frac{P_1}{P_2} \right) \right]^{-1}$ , the height difference between P1 and P2 have to be identical to the FWHM, and we have done in that way as we explained in our response to comment 11. Since the SABER has a better vertical resolution than MLS, we can find representative height where the FWHM can estimate the temperature by using finer height bin size. If we used height bin size comparable to the FWHM instead, we have to assume that FWHM estimate atmospheric temperature near the meteor peak height as Lee et al., (2016) did using MLS.
- In this study, we started with calculation the layer mean temperature having a height bin of 2.4 km and further analyses were conducted.

15. Page 8, Line12: As stated above, it is misleading now. Further the statement in Page 1, Lines 11-13.

- We're very sorry to say this but, we don't understand where misleading part is. Page 8 line12 and page1 line11-13 tell the exactly same feature that the FWHMs have the best correlation with the temperature at around 87 km, which is a little lower than the meteor peak height (~90 km). We also pointed out that rapid decrease in correlation coefficients above MPH is caused by the MHC effect. You can easily find above description in figure 3 in the manuscript.

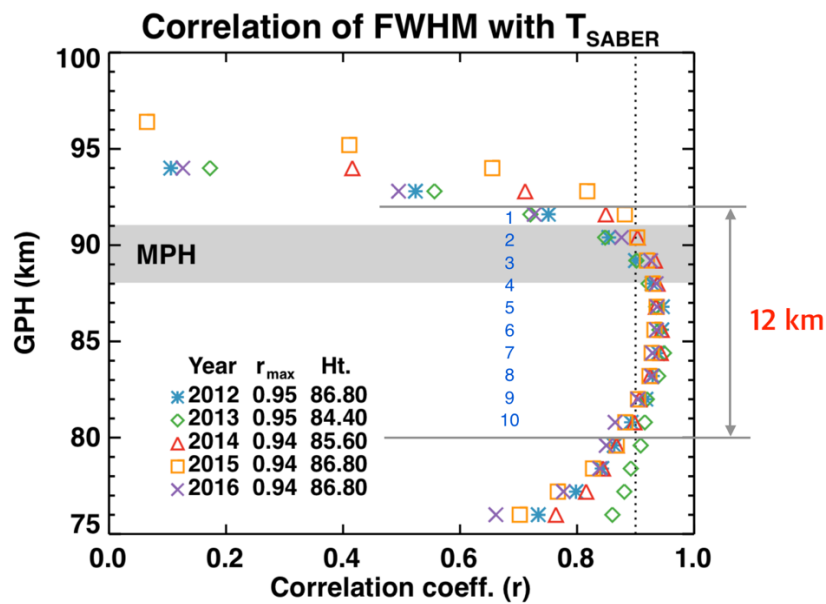
16. Figure 2: the vertical axis of left panel listed MLS, no points in the panel.

- Yes. We admit that MLS data was not used in this study, but we just want to show that SABER has less number of available data compared to MLS due to its limited geometrical coverage for high-latitude (> 52 degrees) regions as

described in the manuscript. This can be used to explain higher fitting error of proportionality constant in least-squares fitting procedure.

17. Figure 3: SABER temperature? Layer mean temperature over FWHM?

- As we described in our response to comment 14, SABER temperature data were interpolated every 1.2 km first and the layer mean temperatures were obtained within 2.4 km height bin. This means the height layer for mean temperature is overlapped by 50 % (height-bin=2.4 km height step=1.2 km). You can find there are 10 data points in 12 km height region in the figure below.



18. This work and Lee et al. [2016] is done with  $TEMPERATURE = C \times FWHM$ , while Liu et al. [2017] adopts  $TEMPERATURE = C \times FWHM + A$ . Liu et al. introduces another term A to fit the relationship between TEMPERATURE and FWHM. Further, Table 1 shows the coefficient, or C, is changing or different in years separately or together, and differs from those in column 4. At last, the authors need clarify what temperature from SABER used, layer mean temperature over FWHM range, or temperature within 2,4 km.

- The linear relationship between the temperature and the FWHM is derived from the basic equations (ideal gas law and hydrostatic equation) and we also showed that the FWHM closely follows background atmospheric pressures ( $P_1, P_2$ ) from independent observations. In this study, we clearly showed the physical meaning of “ $T=C*FWHM$ ” and C should be considered as the constant over 5-year observational period under a given uncertainty.
- When we used “ $T=C*FWHM+A$ ” form as Liu et al. (2017) did to define the relationship between FWHM and the SABER temperature, both C and A

dramatically changes for each year and they are unpredictable as summarized in the table below. What if we have to estimate the mesospheric temperature using “ $T=C*FWHM+A$ ” in 2016 or 2017 ? We can easily expect that independent temperature measurement from the MLS or SABER is necessary to find new C and A in a given period.

Year	C	A
2012	$15.11 \pm 0.03$	$16.52 \pm 0.35$
2013	$17.23 \pm 0.04$	$-5.11 \pm 0.45$
2014	$13.67 \pm 0.03$	$36.71 \pm 0.31$
2015	$11.82 \pm 0.03$	$55.08 \pm 0.30$

Dear Referee #2

We greatly appreciate your constructive comment for thoughtful evaluations of the manuscript and helpful suggestions for its improvement. We did our best to response to all your comments. Author's responses were written in blue text below every referee's comment.

This paper clearly presents an evaluation of a method for estimating atmospheric temperature near the mesopause using the heights of meteor radar detections. As such, the content is of scientific interest and worthy of publication. The writing is clear with a few small grammatical errors that will be easy to correct. The figures are clearly presented and are integrated well with the text.

There are, however, some problems with missing references and poorly described processes that are not fully justified in the text. It is my recommendation that the paper be published following minor revisions.

Overall, it should be noted that while the authors are inferring an estimate of MLT temperature from the width of the meteor radar detection zone, the most directly related parameter is the density scale height. A discussion of the role of scale height on the vertical extent of meteor trails is curiously absent from the manuscript. This was first discussed by Eshleman, 1957 and was investigated in detail in Younger's publicly available 2011 PhD thesis, which the lead author is familiar with.

- We agree that it is very important to mention about density scale height. From the ideal gas law and hydrostatic equation as shown from Eq(1) to Eq(3), scale height ( $mg/kT$ ) should correspond to  $\ln(P_1/P_2)/FWHM$  because we can readily derive the simple formula from ideal gas law and hydrostatic equation as below,

$$\ln \frac{P_1}{P_2} = \frac{mg}{kT} (Z_2 - Z_1)$$

As described in the manuscript,  $Z_2 - Z_1$  is identical to the FWHM.

- Since we defined layer mean temperature  $\langle T \rangle$ , the height region of interest in this study can be considered isothermal. In the manuscript, the ideal gas law was written as  $P = \rho RT$  instead of  $P = nkT$ . According to your comment, we added description of the scale height in temperature estimation from the height width of meteor distribution with relevant references. (Eshleman, 1957; Younger, 2011).

General: The authors neglect the significant effect that meteoroid velocities have on determining the FWHM of the meteor height distribution. Faster meteors will have a smaller FWHM and are more susceptible to high-altitude cutoff. Furthermore, the relative numbers of different velocity meteoroids changes with time of day and season for a fixed observation location. Thus, the authors should calculate FWHM for a number of velocity bins and construct a fitted value for a single representative velocity, say, 30- 35 km/s.

- We totally agree with your comment and we'll calculate FWHM from representative meteor velocity like 30-35 km/s after we check the dependence of the FWHM on meteoroid speed.

General: The asymmetry of the meteor detection height distribution is due primarily to the high-altitude cutoff. What is the effect of using the standard deviation of heights calculated separately above and below MPH?

- Although we have not calculated standard deviation of heights separately above and below MPH, we obtained separate height widths from meteor detection region below and above MPH by independent Gaussian curves to height regions. That means the FWHM can be expressed as sum of half widths of two fitted curves. Unfortunately, the FWHM from two separated height widths gave us worse temperature estimation compared to the FWHM from a unified Gaussian fitting curve or even to traditional meteor decay method. As the figure 1 in Lee et al. (2016) clearly shows, the magnitude of asymmetry in meteor height distribution is very small.

Page 1, line 18-19: Here and throughout the paper, the authors state that they are measuring the mesopause temperature, but what is actually being estimated is a temperature near the mesopause. The height of the mesopause varies substantially more than the meteor peak height for which the authors state that their estimates are representative of.

- According to your comment, we changed “mesopause temperature” to “ temperature near the mesopause”. Thanks.

Page 1, line 18-25: The authors should include some references to general meteor radar operation, such as McKinley, 1961, Ceplecha et al., 1998, or Holdsworth et al., 2004 (Radio Science). Furthermore, a discussion of meteor radar temperatures is incomplete without reference to Tsutsumi et al., 1994 (Radio Science) and Hocking, 1999.

- Following your comment, we added all references in radar operation and meteor radar temperature description. Thanks.

Page 1, line 28-30: The authors fail to acknowledge the theoretical foundation of Eshleman, 1957, which provides the basis for their link between the height range of detected meteors and density scale height, and thus approximate temperature.

- We added statement “Eshleman [1957] provided a theoretical basis for the relationship between the atmospheric density scale height and the height range of detected meteor echoes. This relationship was developed by showing that the width of the height distribution of detected meteors is a nearly linear function of the density scale height [Younger 2011].” based on your comment.

Page 2, line 5-6: The authors should cite a paper describing the meteor radar response function, such as Cervera and Reid, 2004 or just the review paper of Ceplecha et al., 1998.

- We cited Cervera and Reid, 2004. Thanks.

Page 2, line 16-22: For a description of what is now a standard design for meteor radars, the authors should include a reference to Jones et al., 1998 for basic concept and Holdsworth et al., 2004 (Radio Science) for the detection and analysis software used by the King Sejong MR.

- According to the comment, we cited Jones et al., 1998 for the configuration of receiver array and Holdsworth et al., 2004 for the meteor radar data analysis.

Page 2, line 29: When the authors say that they limit phase error to less than six degrees, do they mean for each of the receiver channels, individual antenna pair combinations, or the array mean?

- Phase error in the manuscript means that mean value of phase difference error for the individual antenna pair combinations. We added description to make it clear. Thanks.

Page 3, line 27: It should be noted that atmospheric density is the determining factor in meteoroid ablation. Pressure is really only relevant in a discussion of diffusion of the meteor trail after formation.

- We agree that density primarily controls meteoroid ablation and pressure is a function of density and temperature from the ideal gas law. When we compared density field derived from Aura/MLS and height width of meteor distribution (FWHM), we found that the FWHM had better correlation with the pressure than the density. Based on this, we think the height distribution of detected meteor echoes is determined by not only density but background temperature.

Page 3, line 25-29: A discussion of meteoroid ablation should include a relevant reference, such as Love and Brownlee, 1999 or Rogers et al., 2005.

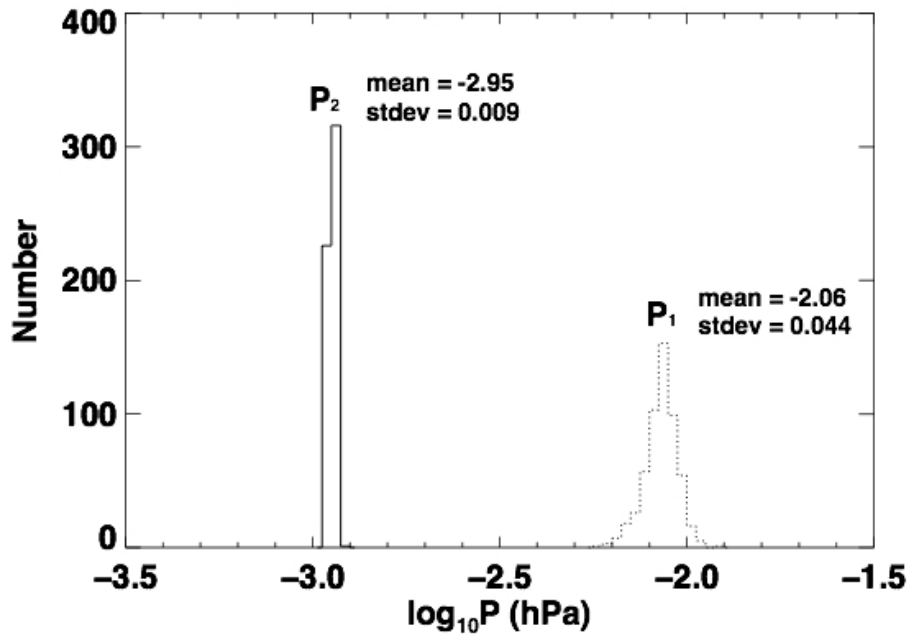
- According to your comment, we added two papers as reference. Thanks.

Page 4, line 1-10: It should be noted that this formulation is only valid for an isothermal atmosphere. This is implied later via the use of  $\langle T \rangle$ , but it should be stated in the derivation. I would like to see how the FWHM compares with the density scale height, which includes a temperature gradient term.

- Once the layer mean temperature,  $\langle T \rangle$  is defined as eq (4), eq (3) can be readily derived by dividing eq (2) by  $\int_{P_2}^{P_1} d \ln P$ . From the FWHM, we can estimate averaged temperature within a layer of two pressure values and the layer mean temperature can define any kind of atmosphere even rapid varying temperature profile. As shown in figure 1, FWHMs well follow constant atmospheric pressure region (P1, P2) and this observationally supports eq (3).

Page 4, general: The authors' derivation and method depends on meteor detections starting and ending at two well defined pressures, P1 and P2, but they do not state why this assumption is valid. Furthermore, they provide no concrete values for P1 and P2 as used in this study and do not provide information on where they obtained these values, although perhaps the reader is meant to infer that SABER values were used? At the very least, the authors should supply the values and uncertainties.

- As Lee et al., (2016) did, we assumed that meteor height distribution is mainly determined by background atmosphere from two independent observations for 5 years such as meteor height distributions from meteor radar and atmospheric pressures from Aura/MLS. To prove this assumption is correct, we used two fundamental equations (ideal gas law, hydrostatic equation) and derived hypsometric equation which obviously showed the linear relationship between the layer mean temperature and the FWHM.
- Based on your comment, we presented 5-year averaged values of P1, P2 with standard deviation calculated from SABER measurements in the manuscript and relevant histogram is added as below,



Page 5, line 9-12: It is worth noting that 92 km is around (and sometimes past) the upper limit of reliable measurements by the MLS instrument. As such, the vertical resolution is less important than the accuracy of values extrapolated from MLS data.

- We agree with your comment, but please note that so many previous studies evaluating temperature [Meek et al., 2013; Kozlovsky et al., 2016; Yi et al., 2016; Lee et al., 2016] and density [Younger et al., 2015; Yi et al., 2018] estimation from meteor radar used MLS temperature/pressure measurements. In this study, we try to find specific height of temperature estimated from the meteor height distribution and this is a main reason why we used SABER data instead of MLS. Because the SABER has better vertical resolution and larger altitude coverage than MLS does.

Page 5, line 17: The authors are comparing a “theoretical” prediction based on C in equation 3, but C itself is derived from experimental observations for the individual radar system. This seems like circular reasoning.

- Firstly, we calculated proportionality constant (C1) between the SABER temperature and the FWHM by least-squares method and C1 should be considered empirical value of proportionality constant. From hypsometric equation, we calculated  $C2 = \frac{g}{R} \left[ \ln \left( \frac{P_1}{P_2} \right) \right]^{-1}$ , which corresponds to proportionality constant, C in eq (3). Although both C1 and C2 represent the proportionality constant between the temperature and the FWHM, they have been derived from independent methods. When we obtained C2 from the

hypsothetic equation, realistic values of (P1, P2) are required and those pressure values were obtained from SABER measurements.

- Based on your comment, we replaced “theoretical values” by “constant in eq (3) with SABER pressure measurements”.

Page 5, line 26: The authors need to provide more detail than “seems plausible”. It would be helpful to compare  $\langle T \rangle$  obtained from their method with an average of SABER values, weighted by the distribution of meteor detections. Given the asymmetry of the meteor height distribution, would this result in a value of  $\langle T \rangle$  corresponding to the lower than MPH maximum correlation height in figure 3?

- Since the FWHM can be defined around the MPH, it is natural to assume that the temperature derived from the FWHM can represent the mean temperature at near the MPH. However, we showed that the representative height of temperature estimated from the FWHM is slightly lower than the MPH by 3-4 km in correlation analysis. We thought that the lower representative height and the asymmetry of the meteor height distribution should be caused by the meteor height ceiling (MHC) effect.

Page 6, line 11: Needs reference. Page 6, line 13-14: This statement should, at the very least, cite Jones, 1995.

- We added Thomas et al., 1988; Steel and Elford, 1991 as references. Jones, 1995 was cited as you commented in line 13-14. Thanks.

Page 6, line 16-17: The destructive interference of backscatter from off-axis portions of the trail is described in detail in Younger, 2008.

- Younger 2008 paper was added in line 16-17. Thanks.

Page 6, line 26: It is not just the reduced electron volume density responsible for reduced backscatter from trails with large initial radii. Backscatter from cylindrically symmetric distributions experiences significant destructive interference past the first maximum of the Bessel function in the backscatter amplitude integral (see e.g. McKinley, 1961 eq. 8-22 or Younger, 2008 figure 2).

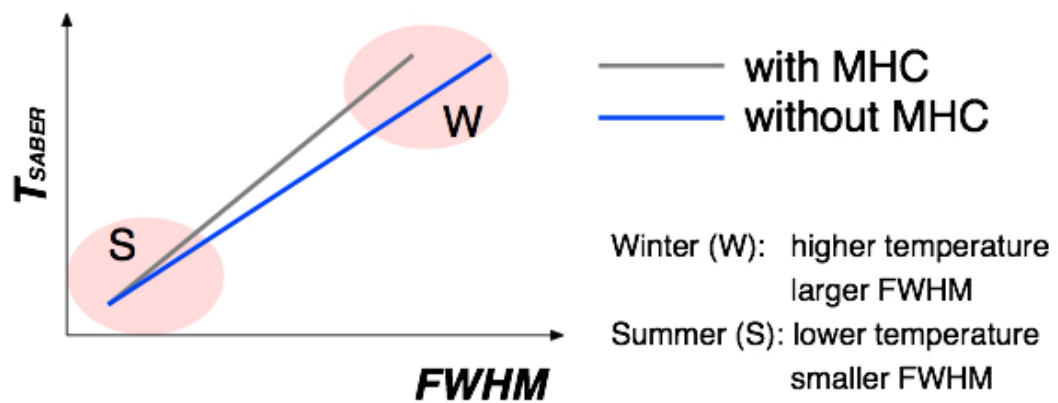
- We're grateful for your comment in Bessel function dependence of backscattered signal amplitude. According to the comment, we corrected the statement as “The reduced electron density and its weighting function (zeroth-order Bessel function) oscillating positive and negative regions with a radial distance in the meteor trail...”

Line 32-33: The precision of the FWHM is a purely statistical quantity determined primarily by the height accuracy of the radar and number of meteors detected. While attenuation terms do determine the behaviour of the high-altitude cutoff in detectability, it does not make sense to invoke attenuation terms in a discussion of the precision of the FWHM term.

- we totally agree with your comment and we modified the sentence to avoid misunderstanding. Thanks. The corrected statement is as follows,
- “Although the background atmospheric pressure field primary factor to determine the FWHM, the MHC also contributes to the FWHM by reducing the detection of high altitude meteor trails.”

Page 8, line 2-4: I fail to see how a demonstration of established meteor radar attenuation theory validates the authors’ temperature estimation technique. The method is validated by correlation with independent measurement techniques. An assessment of attenuation coefficients is valuable for describing the shape of the meteor detection height distribution, but does not validate the method.

- As we described in the last paragraph in page 7 with figure 4 and figure 5, the MHC effect is mainly controlled by initial radius factor. From the relationship between neutral density (molecular mean free path) and initial radius, the MHC mostly occurs within a fixed mean free path supporting previous studies.
- Since the MHC produces asymmetric structure in meteor height distribution due to the high-altitude cutoff in detectability and this means that the MHC decreases the FWHM in meteor height distribution. As shown in table 1, proportionality constants (C1) from the least-squares method using SABER temperature and the FWHM tend to be slightly larger (by 1.4 ~ 3.7 %) than values (C2) from eq (3) with SABER pressure measurements. We thought that underestimated FWHM under the MHC effect provided the reason why C1s are systematically larger than C2 over the entire observation period.
- It should be noted that the MHC reduce the FWHM more effectively in winter when broader meteor height distributions (larger FWHMs) appear than summer because the upper part of FWHM in winter easily reaches cutoff height (~97 km) of MHC. This makes the empirical slope (C1) larger as shown in the figure below,



- In summary, although the MHC affects the absolute value of the FWHM and produces lower representative height of temperature estimation, it well reflects background atmospheric condition because it only happens at a constant atmospheric density (or mean free path).

Figure 2: Label text in the plot area is too small to be legible.

- We used bigger label text for legibility in figure 2. Thanks.

Figure 4: This figure would be improved if the authors also showed the cumulative attenuation coefficient (product of all 3).

- We added the normalized cumulative attenuation coefficient in the right hand. Thanks.

# **Meteor echo height ceiling effect and the mesospheric temperature estimation from meteor radar observation**

Changsup Lee<sup>1</sup>, Geonhwa Jee<sup>1</sup>, Jeong-Han Kim<sup>1</sup>, and In-Sun Song<sup>1</sup>

<sup>1</sup>Korea Polar Research Institute, Incheon, South Korea.

Corresponding author: Changsup Lee ([cslee@kopri.re.kr](mailto:cslee@kopri.re.kr))

## **Key Points:**

- Representative altitude of temperature estimated from FWHM is slightly lower than meteor peak height by about 2-3 km.
- MHC creates remarkable asymmetry in the height profile of the correlation between the FWHM and layer-mean temperature.
- The state of the background atmosphere is intrinsically reflected in the MHC and therefore in the observed FWHM.

## **Abstract**

The mesospheric temperature estimation from meteor height distribution is reevaluated by using the Sounding of the Atmosphere using Broadband Emission Radiometry (SABER) and the King Sejong Station meteor radar observations. It is found that the experimentally determined proportionality constant between the full width at half maximum (FWHM) of the meteor height distribution and temperature is in remarkable agreement with theoretical value derived from the physics-based equation and it is nearly time-invariant for the entire observation period of 2012-2016. Furthermore, we newly found that the FWHM provides the best estimate of temperature at slightly lower height than the meteor peak height (MPH) by about 2-3 km. This is related to the asymmetric distribution of meteor echoes around MPH, which is known to be caused by the meteor echo height ceiling effect (MHC). At higher altitude above MPH, the meteor detection rate is greatly reduced due to the MHC and the cutoff height for this reduction follows a fixed molecular mean free path of the background atmosphere. This result indicates that the meteor height distribution can be used to estimate the mesospheric temperature even under the asymmetric meteor echo distribution caused by the MHC at high altitude.

## 1. Introduction

Recent advances in the performance of meteor radar have enabled continuous observations for the daily **mesospheric** temperature and hourly neutral winds in the mesosphere and lower thermosphere region. As meteoroids enter the earth's atmosphere, they undergo ablation due to collisional heating with atmospheric constituents, leaving cylindrical ionized meteor trails behind them. By observing these meteor trails with a meteor radar, one can extract a variety of essential information on the background atmosphere as well as the meteors [McKinley, 1961; Ceplecha et al., 1998; Holdsworth et al., 2004]. While the neutral winds can be directly obtained from the measurement of Doppler shift of backscattered signals, **the temperature near the mesopause region** has been conventionally estimated from the diffusion coefficients of underdense meteor echoes based on the dependence of the diffusion coefficient on the atmospheric temperature and pressure [Tsutsumi et al., 1994; Chilson et al., 1996; Kim et al., 2012, and references therein]. However, Eshleman [1957] **provided a theoretical basis for the relationship between the atmospheric density scale height and the height range of detected meteor echoes. This relationship was developed by showing that the width of the height distribution of detected meteors is a nearly linear function of the density scale height** [Younger, 2011]. Lee et al. [2016] demonstrated that there exists a clear linear relationship between the full width at half maximum (FWHM) of the height distribution of detected meteor echoes and the temperature retrieved from the Aura Microwave Limb Sounder (MLS) based on a basic theory and observations. They further showed that the temperature estimated from this relation is in better agreement with satellite temperature measurements compared with conventionally estimated temperature from meteor decay times. Although it was successfully shown that meteor height

distribution provides mesospheric temperature, the MLS temperature data has a poor height resolution ( $\sim 10$  km), which is nearly comparable to the FWHM in the mesosphere. Therefore, the resulting temperature from the FWHM was assumed to be a layer mean temperature at near the meteor peak height (MPH). Furthermore, a meteor radar has a limitation on the height range of meteor detection; it depends on radar specifications such as a pulse repetition frequency and a radio wavelength [Cervera and Reid, 2004].

In this study, we reexamine the temperature estimation procedure from the FWHM with the emphasis of the invariance of proportionality constant between the FWHM and background temperature not only from theoretical consideration but also from meteor radar and TIMED/SABER observations. In addition, we also evaluate the validity of temperature estimation from the FWHM under the meteor echo height ceiling effect (MHC). Section 2 describes a theoretical derivation of the linear relationship between the FWHM and background temperature. The results of this study are presented in section 3 with relevant discussions. Finally, this is followed by a conclusion in section 4.

## 2. Observations

### 2.1 King Sejong Meteor radar

Meteor radar has been used to continuously monitor atmospheric winds and temperatures in the mesosphere and lower thermosphere for several decades. Korea Polar Research Institute (KOPRI) has been operated a meteor radar at King Sejong Station (KSS) in Antarctica (62.22°S, 58.78°W) in collaboration with Chungnam National University, Korea, since March 2007. The KSS meteor radar using a frequency of 33.2 MHz transmits 7.2 km width, 4-bit complimentary coded circularly polarized pulses at a pulse repetition frequency of 440 Hz. The transmitter has a peak power of 12 kW and a duty cycle of 8.4%. The receiver is composed of two perpendicular interferometric baselines **as a standard antenna configuration [Jones et al., 1998]** to determine the angle of arrival of backscattered signal from meteor trails [Holdsworth et al., 2004; Lee et al., 2013].

It collects underdense meteor echoes within a horizontal radius of about 250 km from the radar site. The number of meteor echoes from the KSS meteor radar reaches up to 40,000 meteors per day in summer but it declines to about 15,000 in winter. The large number of meteor echoes enables us to obtain reliable meteor samples even beyond the typical meteor detection height of 80-100 km with a better temporal resolution.

In this study we used 5-year-long meteor radar data from 2012 to 2016 to ensure better statistics of meteor distribution even under the minimized meteor detection rate in winter.

**Phase difference error of meteor echo derived from 6 receive antenna pairs** is limited to be less than 6-degree to determine the most accurate meteor height distribution. In deriving a linear relationship between the width of meteor height distribution and the SABER temperature, the geometric height of meteor echoes was converted to

geopotential height to correctly compare with the proportionality constant derived from the fundamental hydrostatic equation.

## 2.2 TIMED / SABER

The Sounding of the Atmosphere using Broadband Emission Radiometry (SABER) instrument is one of four instruments on NASA's TIMED (Thermosphere Ionosphere Mesosphere Energetics Dynamics) satellite to measure the limb emission in the ten broadband infrared channels covering from 1.27  $\mu\text{m}$  to 17  $\mu\text{m}$ . The profile of kinetic temperature is obtained from the 15  $\mu\text{m}$  radiation of  $\text{CO}_2$  from 15 km to 120 km altitude. The SABER instrument views the atmospheric limb perpendicular to the satellite orbital track in an altitude of about 625 km and an inclination of 74°. In order to keep the SABER instrument on the anti-sunward side, the TIMED satellite performs yaw maneuvers about every 60-day period. Consequently, the latitude coverage on a given day extends from about 52° in one hemisphere to 83° in the other and this results in only six months of SABER data available every year in high latitude regions above 52°. The height resolution of the data varies with altitude and it is about 0.37 km in the region of meteor detection. The SABER data used in this study are version 2.0, which includes non-LTE temperature inversions in the upper mesosphere and lower-thermosphere due to the departure from LTE in the  $\text{CO}_2$  15  $\mu\text{m}$  vibration-rotation band for the kinetic temperature determination above 70 km altitude [Mertens et al., 2001; 2004]. The SABER temperature and geopotential height data were restricted to the distance of less than 500 km from the location of KSS to directly compare with the FWHM derived from meteor radar observations during the period of 2012-2016.

### **3. Theoretical Consideration of FWHM and temperature**

According to Lee et al., [2016], most of the observed underdense meteor echoes show specific height distributions being primarily determined by background atmospheric pressure. Figure 1 shows the MPH (blue open squares) and FWHM (red-shaded area) obtained from the fitting procedure with a Gaussian curve applied to the daily meteor height distribution from 2012 to 2016. The background atmospheric pressure field from the MLS measurement is also presented by solid line contours. It is important to note that the MPH closely follows the constant pressure level and a fixed portion of the height distribution (i.e., FWHM) of observed meteor echoes exists within two constant pressure levels around the MPH as shown in Figure 1. As meteors penetrate into the Earth's atmosphere down to about 120 km height, they produce meteor trails, which are composed of metallic ions and electrons by collisions with atmospheric constituents [Love and Brownlee, 1991; Rogers et al., 2005]. This collisional heating process is critically affected by background atmospheric pressure which is a function of density and temperature. Therefore, the height distribution of meteor echoes, represented by the FWHM, is determined by the state of the background atmosphere.

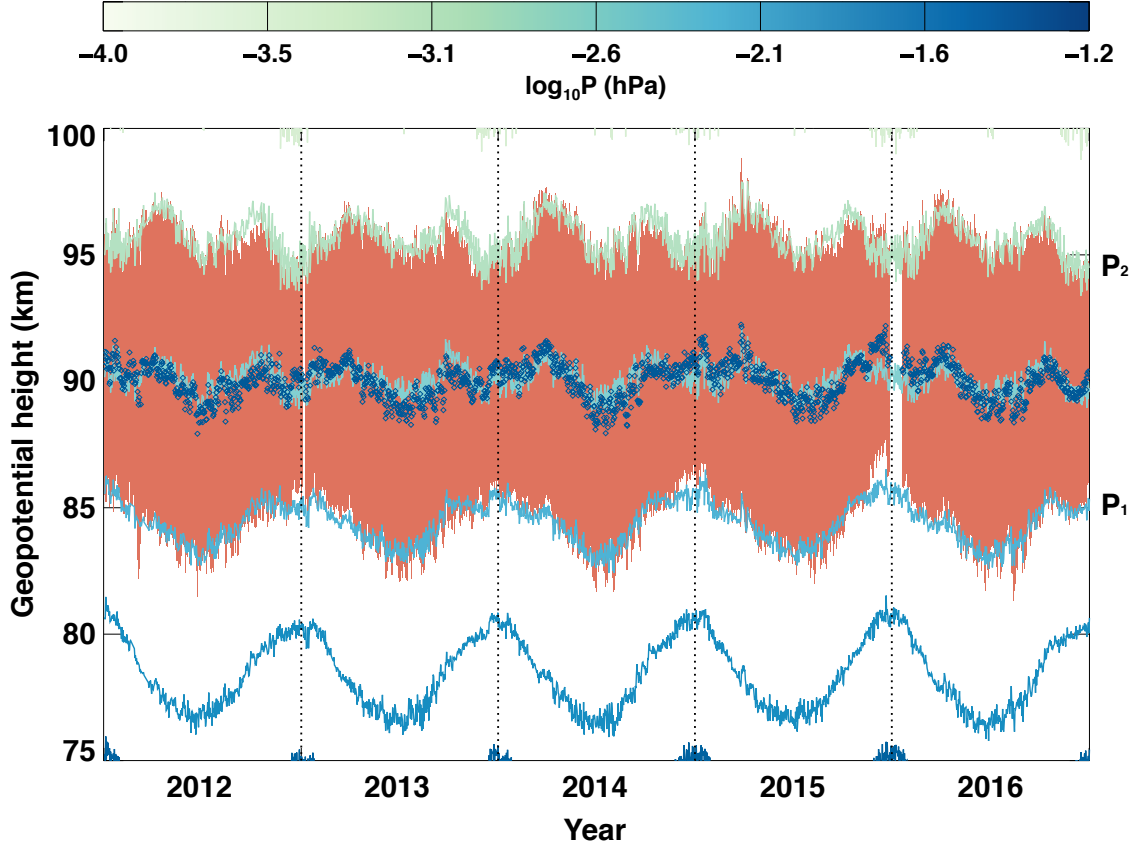


**Figure 1.** Temporal evolution of constant pressure surfaces of the neutral atmosphere from Aura MLS (both filled and line contours) and meteor peak detection heights (blue open diamond) with full width at half maximum (FWHM) of meteor height distribution (red shaded area) from meteor radar observations at King Sejong Station, Antarctica in 2012-2016. Two constant atmospheric pressure (P1, P2) levels being strongly correlated with the FWHM are also presented.

The linear relationship between the FWHM and temperature can be derived from the conventional atmospheric statics: the variation of pressure with height can be determined from the ideal gas law and the hydrostatic equation [Andrew et al., 1987]:

$$\frac{\partial \ln P}{\partial z} = -\frac{g}{RT}, \quad (1)$$

where  $g$  and  $R$  are the gravitational acceleration and gas constant, respectively. After a simple rearrangement for separation of variables, both sides in the equation (1) can be

integrated over the region between two given constant pressure levels of  $P_1(Z_1)$  and  $P_2(Z_2)$  to obtain the hypsometric equation:

$$Z_2 - Z_1 = \frac{R}{g} \int_{P_2}^{P_1} T d \ln P. \quad (2)$$

The height difference  $Z_2 - Z_1$  in equation (2) corresponds to an atmospheric layer between the two constant pressure levels. Since the FWHM of the meteor height distribution nearly coincides with the atmospheric layer as in Figure 1, it can be used to estimate the mean temperature of the layer from the equation (2):

$$\langle T \rangle = C \cdot \text{FWHM} \quad (3)$$

where  $\text{FWHM} = Z_2 - Z_1$  and the proportionality constant  $C = \frac{g}{R} \left[ \ln \left( \frac{P_1}{P_2} \right) \right]^{-1}$ . Here the layer mean temperature is defined as:

$$\langle T \rangle = \frac{\int_{P_2}^{P_1} T d \ln P}{\int_{P_2}^{P_1} d \ln P} \quad (4)$$

As is revealed from the definition of the layer mean temperature given by Equation (4), the mean temperature can be defined for any kinds of temperature profiles even vertically rapidly varying temperature structure in atmosphere.

Equation (3) clearly shows that the neutral temperature near the meteor peak height can be determined by FWHM alone with a proportionality constant. The constant can

empirically be determined based on a linear relationship between the observed FWHM and temperature. It turns out that the determined proportionality constant does not vary with time and can be considered to be a ‘constant’ over the entire observation period. The constant can also be estimated with pressure measurements from SABER observations. **From 5-year averaged values of  $\log_{10} P_1 = -2.07 \pm 0.044$ ,  $\log_{10} P_2 = -2.95 \pm 0.009$  from the SABER pressure measurements during the period of 2012-2016, the ratio between two pressure levels,  $P_1/P_2$  is determined to be 7.59.** Then the proportionality constant in equation (3) can be estimated to be about 16.28 when the gravitational constant  $g$  and gas constant  $R$  are approximately 9.47 and 287.06, respectively, in the region of given pressure levels of  $P_1$  and  $P_2$  near 90 km altitude. In the following section, we will empirically determine the constant using the measurements of FWHM and temperature and will compare it with the estimated constant from the pressure measurements.

## 4. Results and Discussions

### 4.1 Empirical estimation of proportionality constant

Using the FWHM and temperature measured from the KSS meteor radar and SABER, respectively, we can determine the proportionality constant during 2012-2016 period. Figure 2 shows the scatter plots of the daily FWHMs derived from the KSS meteor radar versus the  $T_{\text{SABER}}$  at around 87 km for a year of 2013 (a) and for the entire observation period of 2012-2016 (b). In contrast to MLS temperature data used in our previous study [Lee et al., 2016], SABER temperature measurements above KSS are only available in its south viewing geometry due to yaw maneuvers about every 60 days. This

observational limitation gives rise to fewer temperature data points available for the determination of proportionality constant, which is why there are few data points in the middle of the scatterplot in Figure 2. Nevertheless, it has a much better height resolution than MLS temperature measurement: the height resolution of SABER observation is about 2 km while the resolution of MLS observation is about 10~13 km, which is almost comparable to the FWHM. This characteristic of SABER observation allows us to find the representative altitude of the estimated temperature from the FWHM [Liu et al., 2017].

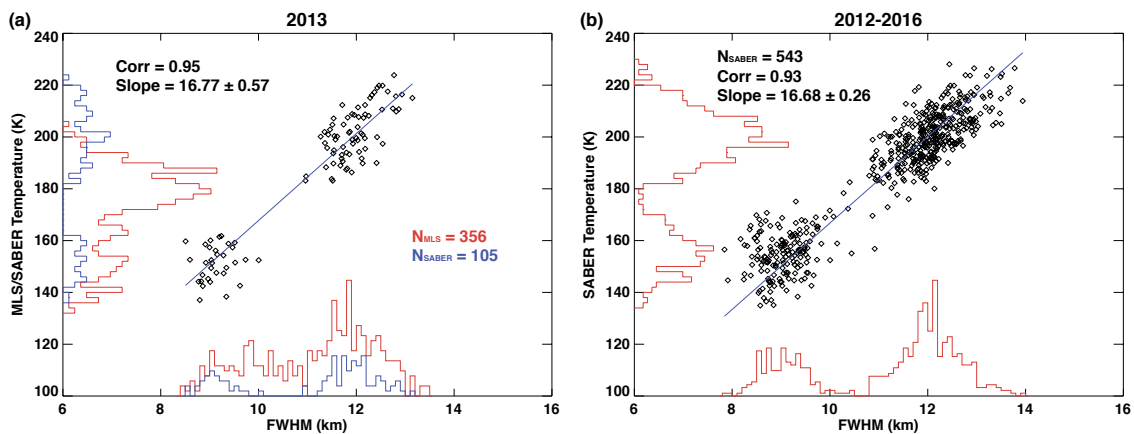


**Figure 2.** Scatter plots of the daily FWHM of the meteor height distribution versus the average value of the SABER temperatures near the mesopause region at King Sejong Station in (a) 2013 and (b) recent 5 years from 2012-2016. The blue solid line depicts the linear regression. The histograms of the two independent temperature measurements from the SABER (blue) and MLS (red) and FWHM data are also presented to show the number of data used in the linear least squares.

There is an obvious linear relationship between  $T_{\text{SABER}}$  and FWHM with notably high correlation coefficients. The slopes in Figure 2 represent the proportionality constant between the FWHM and  $T_{\text{SABER}}$ . Table 1 shows yearly slopes during the 5-year observation period. Note that the slopes are almost invariable within the associated error ranges during the entire observation period of 2012-2016. They also agree well with **the**

**proportionality constant** in equation (3) with SABER pressure measurements. Lee et al. [2016] using the Aura/MLS temperature data obtained notably smaller slope value of 15.71 with a worse correlation coefficient between the FWHM and temperature, which might be due to the poor height resolution of MLS temperature data in the MLT region. It should be emphasized that the essential point of this procedure is the invariance of the proportionality constant between the FWHM and temperature near the MPH. Therefore, once it is determined from the independent measurement of temperature, it can be used to estimate the temperature from the meteor radar observation of the FWHM alone without any additional assumed parameter.

**Table 1.** Slope values and correlation coefficients exhibiting a linear relationship between the SABER temperature and the FWHM from the meteor radar at KSS from 2012 to 2016.

Year	Number of data	Slope	$\frac{g}{R} \left[ \ln \left( \frac{P_1}{P_2} \right) \right]^{-1}$	Correlation coefficient
2012	112	$16.56 \pm 0.51$	16.17	0.95
2013	105	$16.77 \pm 0.57$	16.29	0.95
2014	109	$16.90 \pm 0.56$	16.29	0.94
2015	108	$16.62 \pm 0.64$	16.09	0.94
2016	109	$16.54 \pm 0.56$	16.31	0.94
2012-2016	543	$16.68 \pm 0.26$	16.28	0.93

#### 4.2 Meteor echo height ceiling effect on the temperature estimation

The estimated temperature using Eqs.(2)-(4) is the mean temperature between the two constant pressure levels as shown in Figure 1 and then it seems plausible that the mean temperature represents the temperature at around the meteor peak height (MPH) for the pressure levels around the FWHM. In order to confirm this representative altitude of the estimated temperature with the FWHM, we performed a correlation analysis between the FWHM and layer mean temperatures at different altitudes. Figure 3 shows the height profiles of the correlation coefficient between the FWHM and SABER temperature during the period of 2012-2016. For this analysis the SABER temperatures were averaged at every 1.2 km height within 2.4 km width to obtain daily layer-mean temperatures for each year. It is clear in the figure that the best correlation occurs at slightly lower height (~87 km) than the MPH (88-91 km) by about 3-4 km. The temperature estimation procedure using the meteor decay times, however, assumed that the representative altitude of the estimated temperature is around the meteor peak height, which is about 90 km altitude [Kim et al., 2012; Meek et al., 2013]. A notable asymmetry in the correlation coefficients around the maximum correlation height is another important feature in Figure 3. The correlation coefficient more rapidly decreases at the altitude above the MPH than below and this indicates that the meteor height distribution above the MPH is not only controlled by the background atmospheric state but other factors must be also involved.

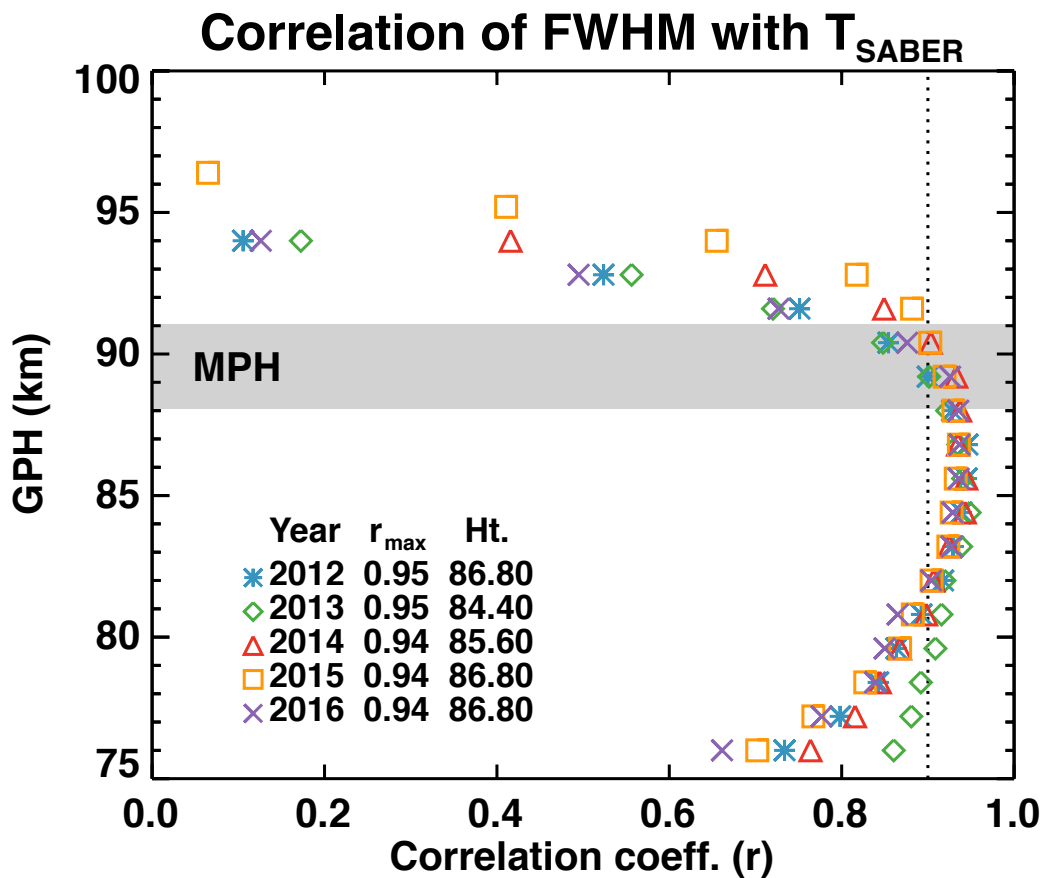


**Figure 3.** The height profile of correlation coefficient of the FWHM and SABER temperatures in 2012-2016. The height information of the maximum correlation coefficient and its value in each year are also summarized. The dotted vertical line indicates a correlation coefficient of 0.9 and the gray shaded box denotes the height range of the MPH variation during the observation period.

The height distribution of meteor echoes detected by meteor radar depends not only on the physical characteristics of meteors and the state of the atmosphere but also on the operational parameters of meteor radar such as a radio wavelength and a pulse repetition frequency. Meteor radar observation shows limited height range of detecting meteors for a given radio wavelength. The backscattered signals from meteor trails beyond this range are significantly attenuated to be detected [Thomas et al., 1988; Steel and Elford, 1991]. This limitation is inherently present in the meteor radar observations, which is known as the meteor echo height ceiling effect (MHC). Immediately after meteor ionized trails are formed, they rapidly expand in a radial direction to reach a finite radial extent called an

initial radius within the interval that meteoric ions are in thermal equilibrium with surrounding atmosphere [Jones, 1995]. As the atmospheric density decreases with increasing height, the initial radius of meteor trail gets increased and becomes greater than a quarter of the radio wavelength, which significantly attenuates echo strength due to the lack of phase coherence from the signals reflected from the different spots in the meteor trail cross-section [Younger et al., 2008]. In general, the meteor trails from fast meteors are produced at higher altitudes and hence meteor radar observation misses the significant part of meteors above certain altitude because of the MHC [McKinley, 1961; Campbell-Brown and Jones, 2003].

According to the echo attenuation theory, there are three major factors controlling the attenuation in the amplitude of meteor echoes from underdense meteor trails. Previous studies reviewed these attenuation factors and quantified their influences on MHC [Thomas et al., 1988; Steel and Elford, 1991]. Since the detailed examination of three attenuation factors is beyond the scope of this study, we only give a brief overview of them and find which one is the most important in meteor echo attenuation. The reduced electron density **and its weighting function (zeroth-order Bessel function) oscillating positive and negative regions with a radial distance** in the meteor trail with a larger initial radius makes backscattered signal too weak to be detected by radars (Initial radius factor,  $\alpha_r$ ) [McKinley, 1961; Younger et al., 2008]. The signal attenuation is also generated by the diffusion during the time of meteor trail formation due to the finite velocity of the meteoroid (Finite velocity factor,  $\alpha_v$ ). If the inter-pulse period of a meteor radar is comparable or longer than the meteor decay times, it is more likely that meteor trail detected by one pulse decays below the threshold of meteor recognition before the

arrival of successive pulse (Pulse repetition rate factor,  $\alpha_p$ ).

In the temperature estimation procedure using the FWHM of meteor height distribution, it is critically important to take account of MHC caused by these attenuation factors on the meteor radar observations. Although the background atmospheric pressure field primary factor to determine the FWHM, the MHC also contributes to the FWHM by reducing the detection of high altitude meteor trails. **It should be noted that proportionality constants derived from least-squares method using the SABER temperature and the FWHM are slightly larger (1.4-3.7%) than values from equation (3) with SABER pressure measurements as shown in Table 1. The underestimated FWHM due to the MHC probably makes systematic difference between two constants over entire observational period.** In this study, we calculated the three attenuation coefficients using key parameters obtained from meteor radar observations to examine how much the FWHM can be affected by MHC and how it can influence on the temperature estimation.

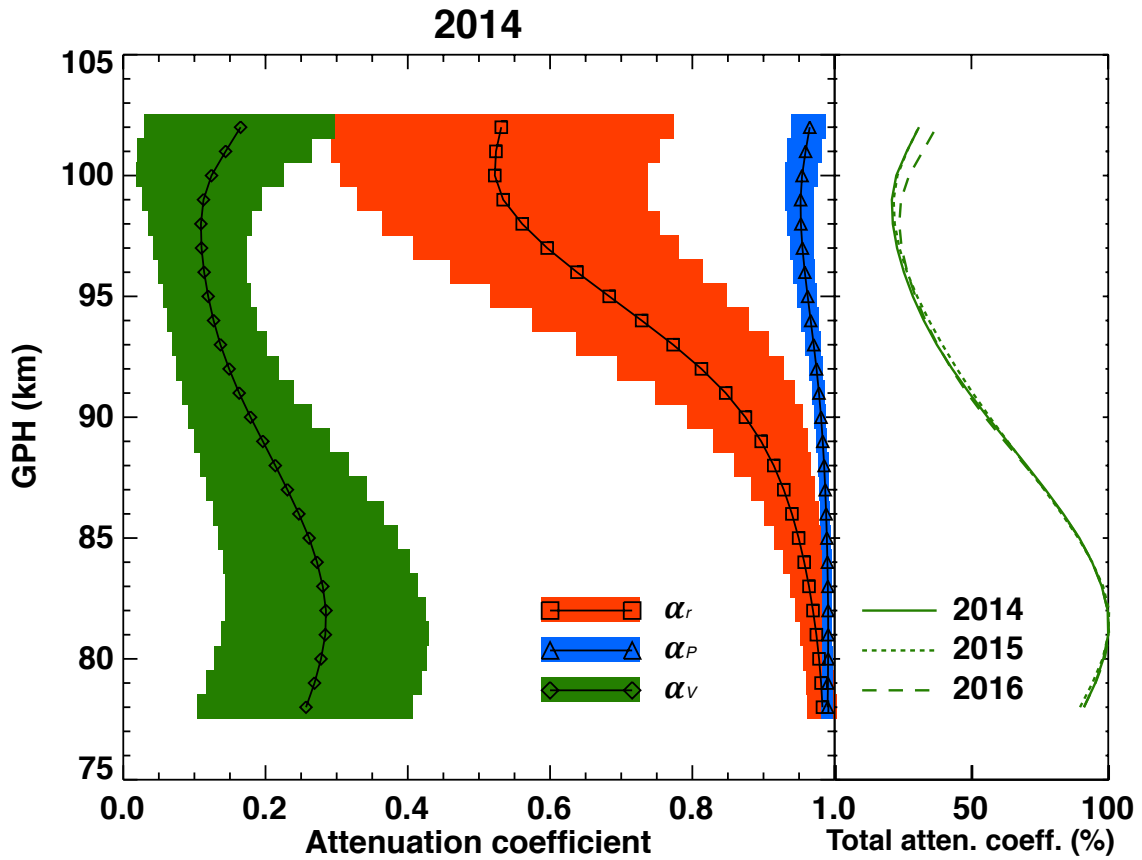


**Figure 4.** (Left) The height variation of yearly mean three attenuation coefficients and their one standard deviations (color-filled horizontal bars) calculated from the KSS meteor radar observations in 2014, (Right) the normalized percentage of yearly mean total attenuation coefficients in 2014-2016.

We applied an attenuation theory described in Steel and Elford [1991] and Ceplecha et al. [1998] to the KSS meteor radar data to calculate the attenuation coefficients. Figure 4 presents the height profiles of three attenuation coefficients with standard deviations calculated from the data in 2014. Because the KSS meteor radar has a large pulse repetition frequency (PRF), the inter-pulse period is much shorter than decay times of most observed underdense meteor trails. Hence, the pulse repetition rate factor (blue filled triangle) should be negligible in the meteor signal attenuation throughout all the altitude region and the net attenuation of meteor echo is dominated by  $\alpha_r$  and  $\alpha_V$  as depicted in Figure 4. The  $\alpha_r$ , in particular, dramatically decreases as the initial radius ( $r_0$ ) increases

with height. This indicates that the amplitude of radar signals scattered from meteor trails is severely declined at higher altitude above about 95 km. As for the finite velocity factor,  $\alpha_v$ , since it is basically related to the background atmospheric state, the height variation of  $\alpha_v$  remarkably coincides with that of meteor decay times, which steadily decreases with height because of the exponential decrease of the background pressure within about 82-97 km altitude range [Singer et al., 2008; Kim et al., 2010]. As shown in Figure 4, the MHC generated by  $\alpha_r$  and  $\alpha_v$  reaches maximum (i.e., minimum attenuation coefficients) at about 100 km and this altitude is known to be a typical cutoff height for 30 MHz meteor radar observation, representing the limitation height of the observation [Olsson-Steel and Elford, 1987; Thomas et al., 1988]. Because of this MHC, signals backscattered from meteor trails are significantly attenuated at higher altitudes, which causes far worse correlations between the height distribution of meteor echoes and the background atmospheric temperatures as shown in Figure 3.

As shown in Figure 4, the MHC for the KSS meteor radar is primarily controlled by the initial radius and finite velocity factors. If we assume that the distribution of meteor speed does not vary much over the 5-year observation period, the two major attenuation processes should mainly be affected by the background atmospheric density. Since the molecular mean free path is inversely proportional to the atmospheric density it is more intuitive to describe the relation between the background atmosphere and the initial radius. Figure 5 illustrates the height distribution of meteor echoes recorded on a single day in 2016 and the height profile of the molecular mean free path calculated from the MLS pressure measurement. Note that the number of meteor echoes observed at a given height bin above the MPH more rapidly decreases with height than below. Jones and Campbell-

Brown [2005] showed that the initial radius of meteor trails is about 1-2 m at the altitude of 95 to 100 km for a meteoroid falling with a speed of 40 km/s and they deduced a relationship between meteor speed  $V$  and the initial radius  $r_i$ :  $r_i \sim V^{-0.2}$ . The molecular mean free path is approximately one-third of the initial radius [Manning, 1958]. When the MHC is most effective at around 97 km altitude (see Figure 5), the mean free path is about a few tens of centimeters with the initial radius of about 2~3 m, which corresponds to approximately a quarter of wavelength of the KSS meteor radar (9.03 m). This indicates that the MHC occurs within a fixed range of mean free path as shown in previous studies (Pellinen-Wannberg and Wannberg, 1994; Westman et al., 2004); in other words, it occurs at a certain atmospheric state. For the KSS meteor radar, the MHC mostly occurs at around 97 km altitude, which exists way above the MPH as shown in both Figure 4 and Figure 5. Consequently, it can be concluded that the MHC affecting meteor height distribution above the MPH is mainly controlled by the background atmospheric condition and in turn, this provides an essential validation of the temperature estimation from the FWHM.

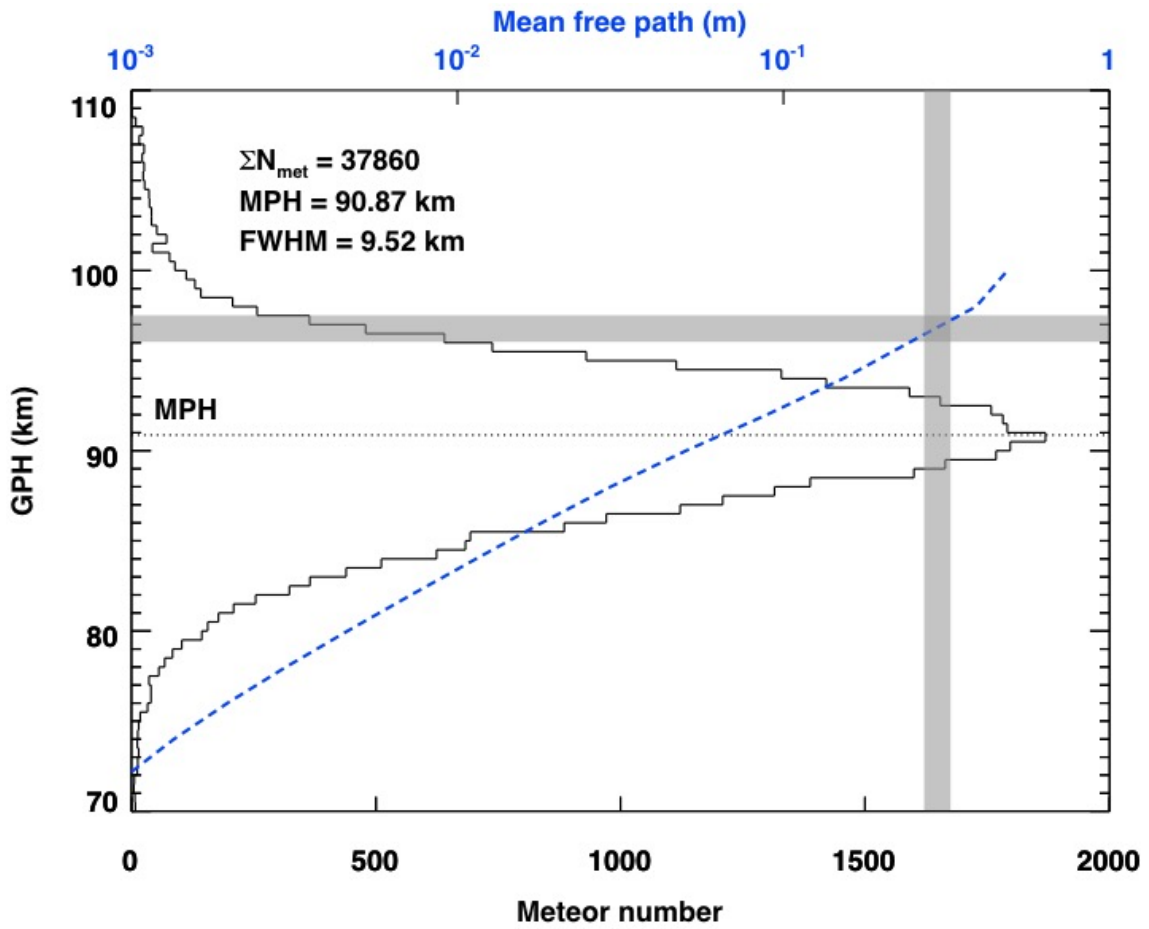


**Figure 5.** The histogram of a meteor height distribution observed by the KSS meteor radar on a single day in 2016 using a 500 m bin. The blue dashed line presents the mean free path of the background atmosphere calculated from the MLS observation. The gray-colored horizontal bar indicates the height layer where rapid decrease in meteor detection rate due to the meteor echo height ceiling appears. The typical range of molecular mean free path that activates meteor echo height ceiling due to the initial radius and finite velocity factors is depicted by a gray-colored vertical bar.

## **5. Conclusions**

In this study, the temperature estimation procedure from the FWHM is reevaluated by verifying the temporal invariance of the proportionality constant between the FWHM and mesospheric temperature over the entire observation period of 2012-2016. Their linear relationship with a proportionality constant is experimentally demonstrated from the SABER temperature and meteor radar observations in the 5-year observation period. The slope of the SABER temperature and FWHM is more consistent with theoretically derived proportionality constant than those from the MLS temperature in Lee et al. [2016]. Compared to the MLS data, much better vertical resolution of the SABER temperature enabled us to find that the mesospheric temperature estimated from the FWHM represent the temperature at around  $87 \pm 2$  km altitude, which is slightly lower than the meteor peak height by about 2-3 km. The lower representative altitude of the estimated temperature results from the asymmetric meteor echo distribution, being much lower meteor detection rates above the MPH, which is caused by the meteor echo height ceiling effect (MHC). Since the MHC well reflects the background atmospheric state, the FWHM derived from the KSS meteor radar can be used to estimate a mesospheric temperature accurately.

## **Acknowledgments**

This study was supported by the grant PE18020 from the Korea Polar Research Institute. The authors would like to thank the TIMED SABER team for providing the kinetic temperature and geopotential height (version 2.0) data. The TIMED/SABER data are available from <http://saber.gats-inc.com/>. The geopotential height and pressure data from the Aura MLS team are also gratefully acknowledged. The Aura/MLS data can be accessed at <http://disc.sci.gsfc.nasa.gov/Aura/data-holdings/MLS>.

## References

- Andrew, D. G., J. R. Holton, and C. B. Leovy (1987), *Middle Atmosphere Dynamics*, 498 pp., Academic, San Diego, Calif.
- Campbell-Brown, M., and J. Jones (2003), Determining the initial radius of meteor trains: fragmentation, *Monthly Notice of the Royal Astronomical Society*, 343(3), 775–780, doi:10.1046/j.1365-8711.2003.06713.x.
- Cepplecha, Z., J. Í. Borovička, W. G. Elford, D. O. ReVelle, R. L. Hawkes, V. Í. Porubčan, and M. Šimek (1998), Meteor phenomena and bodies, *Space Science Reviews*, 84(3), 327–471.
- Cervera, M. A., and I. M. Reid (2000), Comparison of atmospheric parameters derived from meteor observations with CIRA, *Radio Sci.*, 35(3), 833–843, doi: 10.1029/1999RS002226.**
- Chilson, P. B., P. Czechowsky, and G. Schmidt (1996), A comparison of ambipolar diffusion coefficients in meteor trains using VHF radar and UV lidar, *Geophys. Res. Lett.*, 23(20), 2745–2748, doi:10.1029/96GL02577.
- Eshleman, V. R. (1957), The Theoretical Length Distribution of Ionized Meteor Trails, *J. Atmos. Terr. Phys.*, 10, 57-72.**
- Holdsworth, D. A., R. J. Morris, D. J. Murphy, I. M. Reid, G. B. Burns, and W. J. R. French (2006), Antarctic mesospheric temperature estimation using the Davis mesosphere-stratosphere-troposphere radar, *J. Geophys. Res.*, 111, D05108, doi:10.1029/2005JD006589.
- Jones, W. (1995), Theory of the initial radius of meteor trains, *Monthly Notices of the Royal Astronomical Society*, 275(3), 812–818.**

**Jones, J., A. R. Webster, and W. K. Hocking (1998), An improved interferometer design for use with meteor radars, *Radio Sci.*, 33(1), 55–65, doi: 10.1029/97RS03050.**

Jones, J., and M. Campbell Brown (2005), The initial train radius of sporadic meteors, *Monthly Notices of the Royal Astronomical Society*, 359(3), 1131–1136, doi:10.1111/j.1365-2966.2005.08972.x.

Kim, J.-H., Y. H. Kim, C. S. Lee, and G. Jee (2010), Seasonal variation of meteor decay times observed at King Sejong Station (62.22°S, 58.78°W), Antarctica, *Journal of Atmospheric and Solar-Terrestrial Physics*, 72(11-12), 883–889, doi:10.1016/j.jastp.2010.05.003.

Kim, J.-H., Y. H. Kim, G. Jee, and C. Lee (2012), Mesospheric temperature estimation from meteor decay times of weak and strong meteor trails, *Journal of Atmospheric and Solar-Terrestrial Physics*, 89(C), 18–26, doi:10.1016/j.jastp.2012.07.003.

Lee, C., Y. H. Kim, J.-H. Kim, G. Jee, Y.-I. Won, and D. L. Wu (2013), Seasonal variation of wave activities near the mesopause region observed at King Sejong Station (62.22°S, 58.78°W), Antarctica, *Journal of Atmospheric and Solar-Terrestrial Physics*, 105, 30–38, doi:10.1016/j.jastp.2013.07.006.

Lee, C., J.-H. Kim, G. Jee, W. Lee, I.-S. Song, and Y. H. Kim (2016), New method of estimating temperatures near the mesopause region using meteor radar observations, *Geophys. Res. Lett.*, 43, 10,580–10,585, doi:10.1002/2016GL071082.

**Liu, L., H. Liu, H. Le, Y. Chen, Y.-Y. Sun, B. Ning, L. Hu, W. Wan, N. Li, and J. Xiong (2017), Mesospheric temperatures estimated from the meteor radar observations at Mohe, China, *J. Geophys. Res. Space Physics*, 122, 2249–2259, doi:10.1002/2016JA023776.**

**Love, S. G. and D. E. Brownlee (1991), Heating and thermal transformation of micrometeoroids entering the earth's atmosphere. *Icarus*, 89, 26–43.**

Manning, L. A. (1958), The Initial Radius of Meteoric Ionization Trails, *J. Geophys. Res.*, 63(1), 181–196, doi:10.1029/JZ063i001p00181.

McKinley, D. W. R. (1961), *Meteor Science and Engineering*, McGraw-Hill, New York.

Meek, C. E., A. H. Manson, W. K. Hocking, and J. R. Drummond (2013), Eureka, 80° N, SKiYMET meteor radar temperatures compared with Aura MLS values, *Annales Geophysicae*, 31(7), 1267–1277, doi:10.5194/angeo-31-1267-2013.

Mertens, C. J., M. G. Mlynczak, M. López-Puertas, P. P. Wintersteiner, R. H. Picard, J. R. Winick, L. L. Gordley, and J. M. Russell III (2001), Retrieval of mesospheric and lower thermospheric kinetic temperature from measurements of CO<sub>2</sub> 15-mm Earth limb emission under non-LTE conditions, *Geophys. Res. Lett.*, 28, 1391–1394.

Mertens, C. J., et al. (2004), SABER observations of mesospheric temperatures and comparisons with falling sphere measurements taken during the 2002 summer MaCWAVE campaign, *Geophys. Res. Lett.*, 31, L03105, doi:10.1029/2003GL018605.

Olsson-Steel, D., and W. G. Elford (1987), The true height distribution and flux of radar meteors, IN: *European Regional Astronomy Meeting of the IAU*, 67, 193–197.

Pellinen-Wannberg, A., and G. Wannberg (1994), Meteor observations with the European Incoherent Scatter UHF Radar, *J. Geophys. Res.*, 99(A6), 11379–11390, doi:10.1029/94JA00274.

**Rogers, L. A., K. A. Hill, and R. L. Hawkes (2005), Mass loss due to sputtering and thermal processes in meteoroid ablation. *Plan. Space Sci.*, 53, 1341–1354.**

- Singer, W., R. Latteck, L. F. Millan, N. J. Mitchell, and J. Fiedler (2008), Radar Backscatter from Underdense Meteors and Diffusion Rates, *Earth*, 102(1), 403–409, doi:10.1007/s11038-007-9220-0.
- Steel, D. I., and W. G. Elford (1991), The Height Distribution of Radio Meteors - Comparison of Observations at Different Frequencies on the Basis of Standard Echo Theory, *J. Atmos. Terr. Phys.*, 53(5), 409–417, doi:10.1016/0021-9169(91)90035-6.
- Thomas, R. M., P. S. Whitham, and W. G. Elford (1988), Response of high frequency radar to meteor backscatter, *J. Atmos. Terr. Phys.*, 50(8), 703–724, doi:10.1016/0021-9169(88)90034-7.
- Tsutsumi, M., T. Tsuda, T. Nakamura, and S. Fukao (1994), Temperature fluctuations near the mesopause inferred from meteor observations with the middle and upper atmosphere radar, *Radio Sci.*, 29(3), 599–610, doi: 10.1029/93RS03590.**
- Younger, J. P., Reid, I. M., Vincent, R. A. and Holdsworth, D. A. (2008), Modeling and observing the effect of aerosols on meteor radar measurements of the atmosphere, *Geophys. Res. Lett.*, 35(1), L15812, doi:10.1029/2008GL033763.**
- Younger, J. P. (2011), Theory and Applications of VHF Meteor Radar Observations, Ph.D. dissertation, University of Adelaide.**
- Westman, A., Wannberg, G., and A. Pellinen-Wannberg, (2004), Meteor head echo altitude distributions and the height cutoff effect studied with the EISCAT HPLA UHF and VHF radars, *Ann. Geophys.*, 22, 1575-1584, <https://doi.org/10.5194/angeo-22-1575-2004>, 2004.